Physica A 419 (2015) 698–706

Contents lists available at ScienceDirect

Physica A

journal homepage: www.elsevier.com/locate/physa

Characterizing Detrended Fluctuation Analysis of multifractional Brownian motion

V.A. Setty [a,*], A.S. Sharma [b]

[a] Institute for Physical Science and Technology, University of Maryland, College Park, MD 20742, USA
[b] Department of Astronomy, University of Maryland, College Park, MD 20742, USA

HIGHLIGHTS

- Our work characterizes a single exponent estimator like DFA when applied to mBm.
- DFA estimates a time averaged Hurst exponent in systems: this assertion is verified.
- We identify parameters that can impact the robustness of DFA.
- Results serve as benchmark for using DFA as sliding window Hurst exponent estimator.

ARTICLE INFO

Article history:
Received 2 May 2014
Received in revised form 3 September 2014
Available online 25 October 2014

Keywords:
Detrended Fluctuation Analysis
Multifractional Brownian motion
Estimated time average Hurst exponent

ABSTRACT

The Hurst exponent (H) is widely used to quantify long range dependence in time series data and is estimated using several well known techniques. Recognizing its ability to remove trends the Detrended Fluctuation Analysis (*DFA*) is used extensively to estimate a Hurst exponent in non-stationary data. Multifractional Brownian motion (*mBm*) broadly encompasses a set of models of non-stationary data exhibiting time varying Hurst exponents, $H(t)$ as against a constant H. Recently, there has been a growing interest in time dependence of $H(t)$ and sliding window techniques have been used to estimate a local time average of the exponent. This brought to fore the ability of *DFA* to estimate scaling exponents in systems with time varying $H(t)$, such as *mBm*. This paper characterizes the performance of *DFA* on *mBm* data with linearly varying $H(t)$ and further test the robustness of estimated time average with respect to data and technique related parameters. Our results serve as a bench-mark for using *DFA* as a sliding window estimator to obtain $H(t)$ from time series data.

1. Introduction

Statistical properties such as trends and correlations of complex phenomena are important in the study of non-equilibrium phenomena such as extreme events. Due to the non-equilibrium nature of complex driven systems, general statistical analysis tools cannot be readily applied to them. Long range dependence (*LRD*) in data is a key feature [1] and is studied in data from diverse physical systems such as temperature records, river flows, heart beat variability, and space weather, [2–11].

Rescaled range analysis (*R/S*) [12] and fluctuation analysis (*FA*) [13] are statistical tools developed to estimate the variability of time series through estimation of Hurst exponent, H [14], a statistic which is directly related to the scaling

* Corresponding author.
E-mail address: svanurag@umd.edu (V.A. Setty).

http://dx.doi.org/10.1016/j.physa.2014.10.016
0378-4371/

in autocorrelation functions, and, also to the fractal dimension of the time series data. While the scaling exponent, H, is equal to 0.5 for uncorrelated white noise, many natural systems demonstrate values close to 0.7 [15].

These techniques, however, fail to estimate H in non-stationary data. More recently, Detrended Fluctuation Analysis (*DFA*) [16], which is widely considered a better technique than either *R/S* or *FA* due to its capability to detrend a time series data while estimating H, making it viable for non-stationary systems. With increased use of *DFA* technique, its limitations in detrending capabilities are evident [17] and there is need for better alternative detrending schemes for data with atypical trends e.g., *trends that are not addressable by polynomial detrending* [18]. In spite of its purported shortcomings, *DFA* is recognized as an efficient Hurst exponent estimation technique because it utilizes detrending to estimate over lesser number of averages than *FA*.

Fractional Brownian motion (*fBm*), a generalization of Brownian motion, is a quintessential theoretical model for the Hurst effect [19]. Since its discovery, there has been an interest in modeling physical systems as *fBm*. However, it was quickly realized that imposing a uniform H over the span of the data is in fact a restricting condition as uniform level of *LRD* in real life data is uncommon. Multifractional Brownian motion (*mBm*) is a generalization of *fBm* relaxing this condition [20], allowing for variable degrees of self-similarity with non-stationary increments i.e., H varies as $H(t)$ over the time span of the data. It should be realized that *mBm* is also multifractal in nature due to multiple fractal dimensions in the system within the time span of the data. Tunability of its local regularity is a valuable property of *mBm*, realizing which there has been increased interest in modeling various geophysical systems as *mBm* [21–23].

Although there is increasing use of DFA as a technique to study LRD in time series data, it is widely recognized that it yields a single Hurst exponent, and thus cannot distinguish between multi-fractal and mono-fractal systems, e.g., between mBm and fBm. In fact most systems exhibit time varying H exponent, but the estimates yield a constant value. Further, previous studies show the effect of data size used on the Hurst exponent [24,25], thus requiring caution in the interpretation of the estimated values. This is in direct agreement with our study of effect of data size on the Hurst exponent estimated by *DFA* in *mBm* data as seen in Section 4.2. Other schemes such as Multi Fractal Detrended Fluctuation Analysis (*MF-DFA*) were proposed [26], though such techniques address the multifractal nature of time series with respect to one fractal dimension at a time and do not provide a solution with respect to estimating the time varying fractal structure of *mBm*. It is apparent that *DFA* and other similar techniques were assumed to locally estimate a time averaged Hurst exponent [27,28]. This assumption underlies estimator techniques with sliding windows. We believe the success of estimating such a time average depends on the assumption of local linearity of the Hurst exponents, and is analyzed in detail in Section 3.

Using *mBm* data generated from linearly varying Hurst exponents, $H(t)$, we show that *DFA* in fact estimates the time average of $H(t)$ and test the dependence of estimated exponent on various data and technique related parameters. The primary motivation for our study is to establish a bench mark for the performance of *DFA* in estimating a time averaged Hurst exponents from *mBm* data, and, identify its limits.

Sections 2 and 3 introduce preliminary ideas of *LRD*, *fBm*, *mBm*, and, *DFA*, and, establish our estimation methodology. The main results of the study and conclusions follow in Sections 4 and 5, respectively.

2. Fractional/multifractional Brownian motion

Long Range Dependence (*LRD*), commonly identified as self-affinity, self-similarity, or long-range persistence, is a statistical property of time series data where the rate of decay of its autocovariance is slower than exponential, and most commonly a power law. This property is usually quantified using the Hurst exponent H (also known as the Hölder exponent), which is measured using *R/S* or the fluctuation analysis (*FA*) technique for stationary data. The Hurst exponent, $H \in (0, 1)$ with increasing value implying increasing *LRD*, and 0.5 as the threshold where the correlations are completely absent.

Fractional Gaussian noise (*fGn*, which is stationary in nature) is proposed as a model for data with *LRD* and fractional Brownian motion (*fBm*) (its non-stationary counterpart) is its corresponding Wiener process generated using *fGn* as its incremental process. A continuous time fractional Brownian motion (*fBm*), $B_H(t)$ with Hurst exponent H is a Gaussian process with zero-mean and is H-self affine i.e.,

$$B_H(\lambda t) \cong \lambda^H B_H(t), \quad \forall\, \lambda > 0. \tag{1}$$

Also, its covariance varies by definition as [29],

$$\mathrm{cov}[B_H(t_1), B_H(t_2)] = \frac{1}{2}(|t_1|^{2H} + |t_2|^{2H} - |t_1 - t_2|^{2H}). \tag{2}$$

Thus, H characterizes the relative smoothness of the resulting Brownian motions. It can also be seen that when $H = 1/2$ and $t_1 > t_2$, $\mathrm{cov}[B_H(t_1), B_H(t_2)] = t_2$, thus it is a Wiener process (Brownian motion). However when $H > 1/2$, then the increments are positively correlated and when $H < 1/2$, the increments are negatively correlated. This means that we have a smooth long-term correlated time series data for when $H > 1/2$ and anti-correlated data for when $H < 1/2$. The increments in a fBm is fractional Gaussian noise (*fGn*) as seen in Eq. (3), and is stationary in nature.

$$G_H(t) = B_H(t + 1) - B_H(t). \tag{3}$$

A problem with *fBm* is that although they capture the self-similarities well, the pointwise irregularity given by the constant Hurst parameter, H, is invariant in time. This restricting condition can be over come by generalizing *fBm* to a

broader class of Brownian motions where the local irregularity is given by a time varying Hurst exponent, $H(t)$, known as multifractional Brownian motion (*mBm*). In order to simulate data with such properties, a time series $B_{H(t)}$ of an *fBm* with a Hurst parameter, $H(t)$ at time t is generated and a time series $W_{H(t)}$ is computed to be equal to $B_{H(t)}$ by interpolation. Each of the *fBm*s can be generated using many methods. In our simulations, we applied the method of circulant matrices [30] to generate each of such *fBm*s with different Hurst exponents. Producing an *fBm* with a stationary *fGn* as its incremental process (as in Eq. (3)) requires a method to filter a typical Gaussian noise of low frequency components to produce a covariance as described in Eq. (2) using Fourier filtering technique. Circulant matrices, which are diagonalized by a discrete Fourier transform allow for faster solutions for linear equations that contain them by fast Fourier transform [31]. Subsequently, the field of *fBms* are interpolated by a krigeage method [32]. The method of kriging predicts intermediate value of a function at a given point by computing a weighted average of the known values of the function in the neighborhood of the point, as against a piecewise-polynomial spline, which based on smoothness may not produce the most likely values for intermediates. This method is known to be reliable in simulating discrete time *mBm* [33,34].

3. Estimation of time averaged Hurst exponent by *DFA*

Detrended Fluctuation Analysis (DFA) is extensively used for analyzing *LRD* in time series data, particularly those with non-stationarities [35]. In this technique, a random walk is created using the time series as is usually done in *FA*, however its departure from traditional fluctuation analysis method arises due to the simultaneous detrending operation performed using a polynomial of known order (p) which is locally fit within a time window of fixed size. *DFA*, thus consists of the following steps: the time series data $X(i)$ of length N is first shifted by its mean $\langle X\rangle$ and its cumulative sum calculated as

$$Y(j) = \sum_{i=1}^{j} [X(i) - \langle X\rangle]. \tag{4}$$

This cumulative sum series, $Y(j)$ is now segmented into time windows of different lengths ΔT, yielding a collection of set of random walks of varying sizes. These random walks are detrended within the windows by locally estimating their trends as best fit polynomials of order p, $Y^{(p)}_{\Delta T}(j)$. These trends are now removed by subtracting them from the cumulative sum data and the resulting fluctuations, generally referred to as fluctuation functions are calculated as the mean squared deviations:

$$F^{(p)}(\Delta T) = \left(\frac{1}{N} \sum_{j=1}^{N} [Y(j) - Y^{(p)}_{\Delta T}(j)]^2 \right)^{\frac{1}{2}}. \tag{5}$$

If the data $X(i)$ have long-range correlations, it would be reflected in the fluctuation functions $F^{(p)}(\Delta T)$, with a power-law:

$$F^{(p)}(\Delta T) \propto (\Delta T)^{\alpha}. \tag{6}$$

The scaling exponent α is calculated (from scaling within DFA) by best fit of log–log plot between $F^{(p)}(\Delta T)$ and window size ΔT using linear regression performed by least squares method. This scaling exponent, α, is related to the Hurst exponent H as: $\alpha = H$ for *fGn* and as, $\alpha = H + 1$ for *fBm* because *fBm* is the cumulative sum or the integral of *fGn*. *DFA* technique applied with a detrending of pth order polynomial is commonly referred to as *DFAp*.

We characterize the performance of *DFA* on systems with time varying H exponents using simulated *mBm* data with linearly varying $H(t)$ in time. The choice of linear $H(t)$ is motivated by the consideration that its time variation will be gradual, and, the system can be treated as piece-wise local linear (in Hurst exponents). This allows one to divide the data into segments in which a time averaged Hurst exponent can be estimated under the local linearity assumption. It should be noted that piece-wise linearity forms the basis for earlier studies [28]. Further, we analyzed systems with a potential seasonal variation in Hurst exponents using *mBm* data with sinusoidally varying $H(t)$ as the standard model [36]. The results of the time averaged Hurst exponent estimated by *DFA* technique were found to be in accordance with results from linearly varying $H(t)$. That is, robustness of H estimated by *DFA* for *mBm* data with a sinusoidally varying $H(t)$ was found to depend on the amplitude and the frequency (of $H(t)$). More specifically, increasing the amplitude or frequency of the sinusoidal variation was found to deteriorate the quality of H estimated by *DFA*. This can be explained by the effect of slope of linear $H(t)$ on the quality of exponent estimated by *DFA* as seen in Section 4.3. Hence, results from linearly varying Hurst exponents can be used to explain results for any other form of $H(t)$ in real life data by using local linearity arguments.

We used Monte Carlo simulations to study the performance of *DFA* when applied to *mBm* data, which is simulated with $H(t) = at + b$ over a time length $t = 1$ to T using the data simulation method described in Section 2. The parameters a and b are chosen to control the range of $H(t) = R = \max_{1\le t\le T} H(t) - \min_{1\le t\le T} H(t)$, and, its mean = $\langle H\rangle_{\text{act}}$. This condition relates various parameters as:

$$\begin{aligned} a &= \frac{R}{T-1}, \quad \text{and} \\ b &= \langle H\rangle_{\text{act}} - \frac{R}{2} - \frac{R}{T-1}. \end{aligned} \tag{7}$$

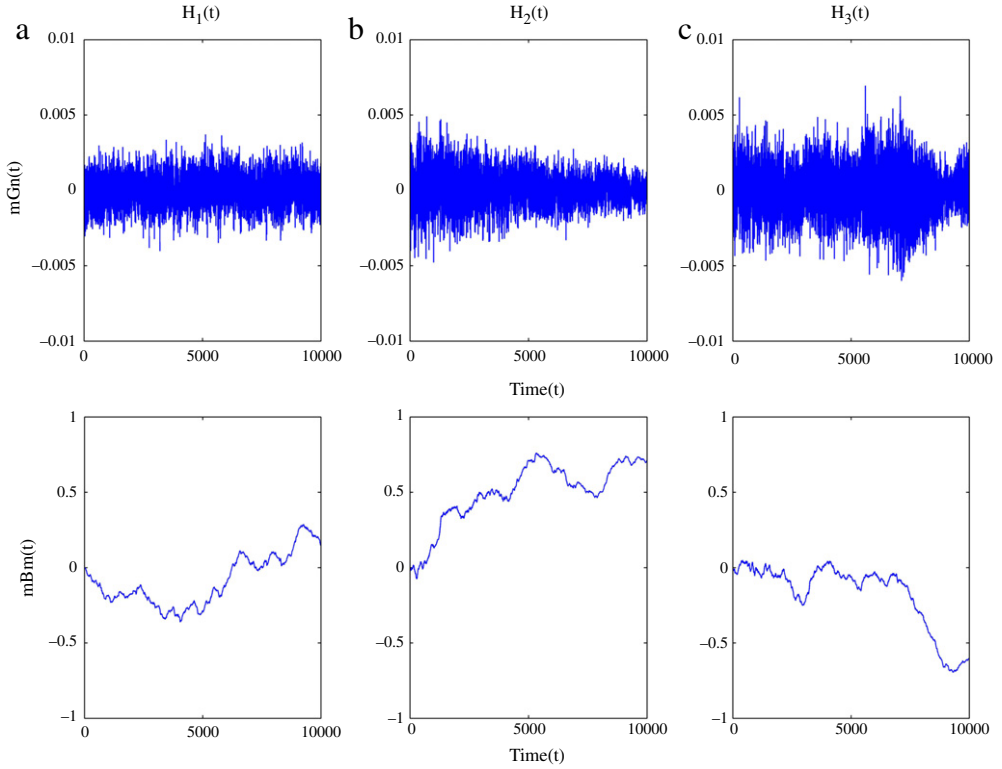

Fig. 1. Simulated data with various forms of $H(t)$ with the incremental process, *mGn* shown in upper panel and the corresponding *mBm* in bottom panel. In (a), $H_1(t) = c = 0.75$. In (b), $H_2(t) = at + b$ with $a = 10^{-5}$ and $b = 0.7$ i.e., $\langle H\rangle_{\text{act}} = 0.75$ and $R = 0.1$. In (c), $H_3(t) = H_2(t) + \epsilon_t$ with ϵ_t drawn from normal distribution, $\mathcal{N}(0, \sigma^2)$ such that $\sigma = \langle H\rangle_{\text{act}} \times 10^{-3}$. It is interesting to note the differences in variability in *mGn* resulting in differences in *LRD* natures of *mBm*.

The time series of the *mBm* is shown in Fig. 1. When $H_1(t) = 0.75$, the *mGn* corresponding to respective *mBm* demonstrates uniform variability as expected. For $H_2(t) = at + b$ with $a = 10^{-5}$ and $b = 0.7$ i.e., $\langle H\rangle_{\text{act}} = 0.75$ and $R = 0.1$, we see that with increasing t, H increases resulting in decreasing variance in *mGn* data thus resulting in increasing *LRD* in *mBm* data when compared to the case in 1(a). In Fig. 1(c), for $H_3(t) = H_2(t) + \epsilon_t$ with ϵ_t drawn from normal distribution, $\mathcal{N}(0, \sigma^2)$ such that $\sigma = \langle H\rangle_{\text{act}} \times 10^{-3}$, we see that due to noise in $H_3(t)$ data, the variance shows no regular pattern in *mGn* and that is reflected in the *LRD* pattern in *mBm*. These figures show us qualitatively the difference in the nature of *LRD* within data with different forms of $H(t)$. If we had no *a priori* knowledge of the time varying nature of a data's Hurst exponent, the differing degrees of *LRD* between data would be viewed assuming a uniform exponent. Similarly, a single Hurst exponent estimation technique such as *DFA* would measure the time averaged exponent, denoted as $\langle H\rangle_{\text{est}}$ which would be equal to $\langle H\rangle_{\text{act}}$ under the ideal condition of $R = 0$ (or $a = 0$). In fact, this assumption constitutes the central hypothesis of this paper.

While measuring for $\langle H\rangle_{\text{est}}$ using *DFA*, we apply linear regression between logarithm of fluctuation function ($F(\Delta T)$) and logarithm of the time window (ΔT), specifically the method ordinary least squares to find the best-fit slope and the standard error of least squares slope [37]. Since we assume *DFA* measures a uniform exponent in the course of this paper, we measure the slope over logarithmically equi-spaced values of time windows, ranging from $\Delta T = 10$ to $\lfloor \frac{T}{10} \rfloor$ (the integer rounded floor value) to eliminate spurious curvatures at lower time windows and also have certain minimum number of samples to obtain the relevant averaged fluctuation function at higher time windows. We denote the standard error as $SE(\langle H\rangle_{\text{est}})$ (shown in error bars in the following figures) which gives us the precision in $\langle H\rangle_{\text{est}}$ estimated by the *DFA* technique. Furthermore, error of estimation of $\langle H\rangle_{\text{act}}$ is measured in terms of relative error of estimation as:

$$EE(\langle H\rangle_{\text{est}}) = \frac{|\langle H\rangle_{\text{est}} - \langle H\rangle_{\text{act}}|}{\langle H\rangle_{\text{act}}}. \tag{8}$$

For some of the sections, we perform ensemble averaging and the resulting $\langle H\rangle_{\text{est}}$ is an average slope over all the ensembles and so is the standard error.

All the following computations were performed on a MATLAB 7.8 platform.

4. Analysis of *DFA* performance

The ability of *DFA* to yield H values intrinsic to a system was tested using the data of *mBm*. The most basic of such tests is to study how close $\langle H\rangle_{\text{est}}$ is to $\langle H\rangle_{\text{act}}$. It is expected that $\langle H\rangle_{\text{est}}$ would be sensitive to various parameters pertaining to the

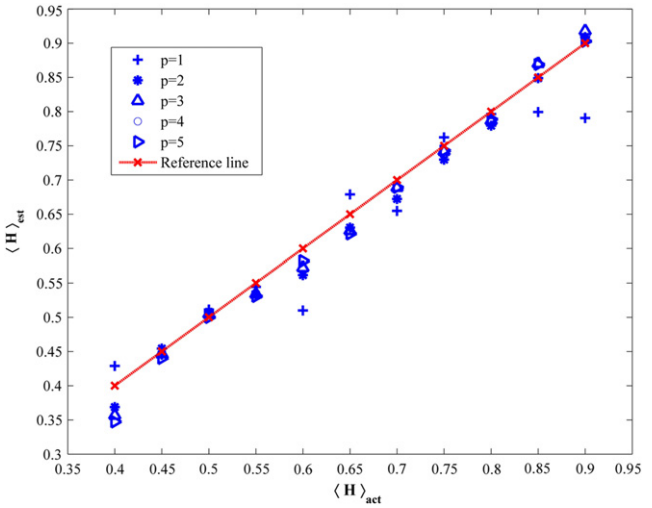

Fig. 2. Dependence of $\langle H\rangle_{\text{est}}$ on the polynomial order (p) of *DFAp* used. The actual average values ($\langle H\rangle_{\text{act}}$) are shown in red. $R = 0.06$ for all $H(t)$ used and $T = 2^{13} = 8192$. We see $p = 1$ has higher *EE* compared to other cases. (For interpretation of the references to color in this figure legend, the reader is referred to the web version of this article.)

technique and of the data. Some of such basic parameters are: p the order of the polynomial, T the length of the data, R the range of $H(t)$, and, possible noise in $H(t)$.

We begin our numerical experiments by first testing to see if $\langle H\rangle_{\text{est}} = \langle H\rangle_{\text{act}}$ whilst simultaneously observing the sensitivity of $\langle H\rangle_{\text{est}}$ to p of *DFA*.

4.1. Time averaged Hurst exponent and its dependence on the order of detrending polynomial, p

The first studies are designed to test how well a single exponent $\langle H\rangle_{\text{est}}$ computed with *DFAp* represents $\langle H\rangle_{\text{act}}$ of the *mBm* data. For our numerical experiment, we chose *mBm* data with $\langle H\rangle_{\text{act}}$ values ranging from 0.4 to 0.9 (steps of 0.05) with $R = 0.06$. This value of R is chosen to assure that we have multifractional Brownian data with a certain minimum varying degree of self-similarity and for other reasons as described in Section 4.3. The simulations are performed on *mBm* of size $T = 2^{13} = 8192$ for one ensemble of the data with no ensemble averaging. This length of the data is chosen keeping in mind the nature of dependence of $\langle H\rangle_{\text{est}}$ on T (discussed in the next section) and also to standardize the computational time.

Fig. 2 shows the dependence of $\langle H\rangle_{\text{est}}$ on $\langle H\rangle_{\text{act}}$ for various detrending polynomial orders (p) of *DFAp* used. For $p = 1, \ldots, 5$, *DFA* yields exponents close to $\langle H\rangle_{\text{act}}$, albeit with varying accuracy. For each $\langle H\rangle_{\text{est}}$, from a *DFA* of order p, we see that there is no regular pattern of increasing/decreasing accuracy with increasing $\langle H\rangle_{\text{act}}$. This also concurs with our expectation that for a fixed R, the extent of *LRD* as measured by $\langle H\rangle_{\text{est}}$ should not be dependent on $\langle H\rangle_{\text{act}}$ of the data.

But for every $\langle H\rangle_{\text{act}}$, we see significant differences with in $\langle H\rangle_{\text{est}}$ from various p. This is expected since lower polynomial orders ($p = 1$, linear) fit worse than higher orders because detrending using a linear fit on non-stationary data is expectedly worse, but this comes with a caveat that this is not necessarily so for higher order polynomials due to poor conditioning, particularly for lower time windows. This may explain why we see that while $p = 1$ results in higher error (lower accuracy) as compared to higher order p, there is no definite trend or difference in error for $p = 2, 3, 4, 5$. So, in the following studies, we use $p = 2$, i.e., a quadratic detrending which is also the most commonly used order.

To further settle on which length of data is appropriate within available computational resources, we proceed to test the effect of T on $\langle H\rangle_{\text{est}}$ in the next section.

4.2. Dependence on data size, T

Although this is not a strict condition, it is important to examine the data size effects on $\langle H\rangle_{\text{est}}$. This prompted us to set up the next experiment where we took various *mBm* data for which $\langle H\rangle_{\text{act}} = 0.75$ and $R = 0.06$ but of differing size T. Fig. 3 shows this dependence of $\langle H\rangle_{\text{est}}$ and the $SE(\langle H\rangle_{\text{est}})$ on the size of *mBm* data (T) used. Just like in the previous case, our result is for one ensemble of the data and so, there was no averaging. We fixed $\langle H\rangle_{\text{act}}$, to make our point in a more clear fashion as showing different $\langle H\rangle_{\text{act}}$ would confuse one and may make it hard to see a clear pattern in $\langle H\rangle_{\text{est}}$.

We see that while longer data sizes do not necessarily effect the accuracy (difference between blue points and the reference line in red in Fig. 3), it does improve the quality of estimation as seen by decreasing error bars—measured by $SE(\langle H\rangle_{\text{est}})$. So, we fixed the length of the data to be $T = 2^{13} = 8192$ for further simulations to assure lower SE.

The results so far help establish a benchmark on p and T, using which we can perform further tests. In the next section, we answer an important question: how R would effect $\langle H\rangle_{\text{est}}$?

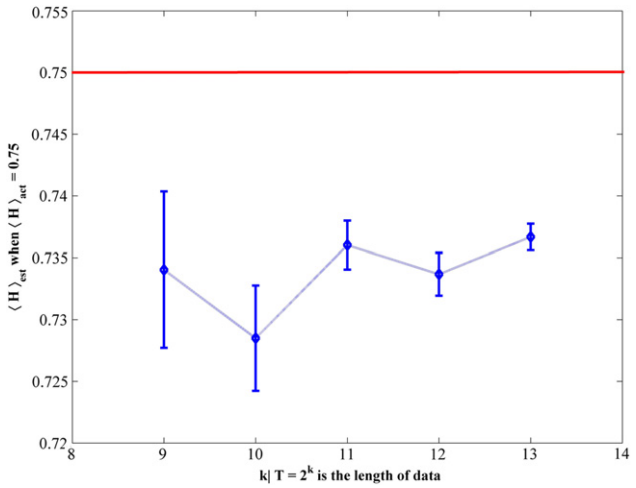

Fig. 3. Dependence of $\langle H\rangle_{\text{est}}$ on the length of data used for $\langle H\rangle_{\text{act}} = 0.75$ and $R = 0.06$. It is interesting to note that while increasing data size has no predominant effect on *EE*, it does improve the quality of performance or decrease the *SE* as shown by error bars. (For interpretation of the references to color in this figure legend, the reader is referred to the web version of this article.)

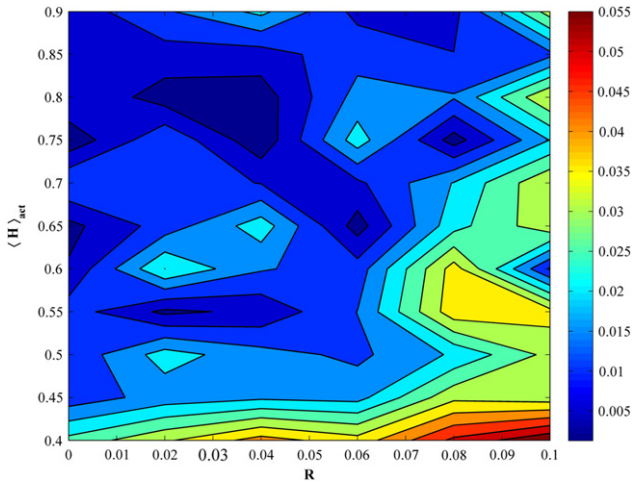

Fig. 4. Contour map showing the dependence of relative accuracy of estimation (legend shown in color map on the right) on $\langle H\rangle_{\text{act}}$ and *R*. We see interesting features emerging from this picture in that data with $\langle H\rangle_{\text{act}} \geq 0.75$ have predominantly lower *EE* compared to other cases, and, $R = 0.06$ serves as a transition point where *EE* increases rapidly beyond 2% approaching 5% near $R = 0.1$. (For interpretation of the references to color in this figure legend, the reader is referred to the web version of this article.)

4.3. Dependence on range R of H(t)

This result is important because in the assumption of a local linear $H(t)$, one would like to know how the slope of the linearly varying $H(t)$ as measured by *R* for fixed *T* and for each $\langle H\rangle_{\text{act}}$, would effect $\langle H\rangle_{\text{est}}$. To test this particular effect, we measure $EE(\langle H\rangle_{\text{est}})$ for data with a $\langle H\rangle_{\text{act}}$ (ranging from 0.4 to 0.9 in steps of 0.05) and *R* (values ranging from 0 to 0.1 in steps of 0.02). This accuracy is plotted on a contour map as shown in Fig. 4. The simulations were performed for 100 realizations of *mBm* data, each of size $T = 8192$ and $\langle H\rangle_{\text{est}}$ is estimated using *DFA* with detrending order $p = 2$. Hence, the resulting *EE* is an average over all the 100 ensembles.

The ensemble averaging is used mainly because our results for a single sample of data were inconclusive. However, a clearer picture emerged as we averaged over several such ensembles. Our results show that there is a generally decreasing trend in accuracy (increasing *EE*) with increasing *R*. This is in line with what we expect when *R* (or the slope *a*) increases with constant data size *T*, worsening performance (or increasing *EE*) of *DFA* in estimating $\langle H\rangle_{\text{act}}$ is expected intuitively. This argument is based upon the premise that when we enforce through the technique to estimate a single exponent from a data with a spread of exponents, we are actually averaging all the different possible Hurst exponents. With increasing *R*, the spread in various possible exponents, or the standard deviation increases and results in worsening accuracy as we are essentially trying to fit a broadly distributed (and possibly skewed) set of exponents to a narrow Gaussian distribution. This results in worsening accuracy, and, we stop the simulations at $R = 0.1$ as this is the point where in general the accuracy starts

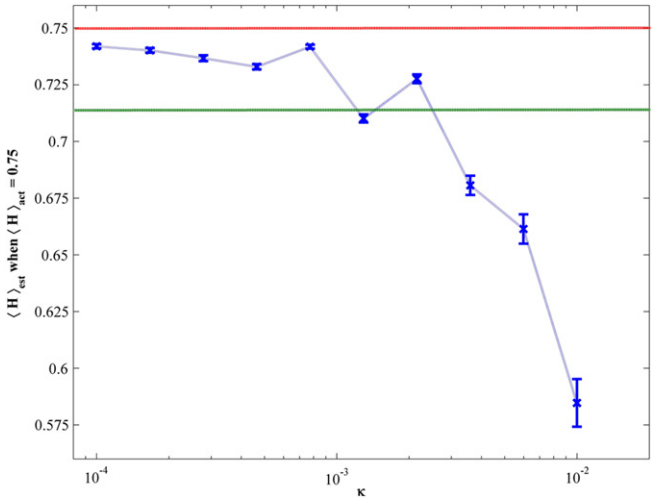

Fig. 5. Dependence of $\langle H \rangle_{act}$ on the strength of Gaussian noise ($\mathcal{N}(0, \sigma^2)$) added to $H(t)$, represented here by $\kappa = \sigma \times \langle H \rangle_{est}$. We note how rapidly *EE* increases, well beyond the 5% limit (as shown in green line) as the strength increases beyond 10^{-3}. (For interpretation of the references to color in this figure legend, the reader is referred to the web version of this article.)

to fall below 95% or $EE \geq 5\%$ (as seen in ratio in the contour colormap in Fig. 5). We chose to use 5% as the limiting condition so as to standardize the benchmarks. Although it might sound arbitrary, this is a meaningful assumption because data that result in higher *EE* would typically show non-convergent behavior in their respective fluctuation plots for *DFA*, making it almost look like there are scaling crossovers which is a different phenomena altogether. Also, this result motivated us to use $R = 0.06$ for our simulations in Sections 4.1, 4.2 and 4.4 since for this value of *R*, although the data is multifractional in principle, with accuracy in estimation over 98% for most $\langle H \rangle_{act}$, the data looks unifractional in the view of the *DFA* technique.

There is another interesting result in Fig. 4 which was not discussed in Fig. 2: with increasing $\langle H \rangle_{act}$, over all *R*, the $EE(\langle H \rangle_{est})$ is in general decreasing till $\langle H \rangle_{act} = 0.75$ and then remains relatively invariant thereafter. This is interesting because it contradicts our earlier conclusion on the dependence of $\langle H \rangle_{est}$ on $\langle H \rangle_{act}$ (Section 4.1). It can be reasoned out that with increasing $\langle H \rangle_{act}$, as the level or correlations i.e., extent of *LRD* is increasing, *DFA* could do a better job estimating $\langle H \rangle_{act}$ with a threshold occurring at $\langle H \rangle_{act} = 0.75$. However, this is an interesting phenomenon because data with $H \geq 0.7$ is known to show predominant *LRD* behavior than the condition $H \geq 0.5$. In data with $\langle H \rangle_{act} \geq 0.75$, and, $R \leq 0.1$, the $H(t) \geq 0.7$, which might imply a change in intrinsic nature of the data as speculated previously [38] when compared with when $0.5 \leq H(t) \leq 0.7$. This intriguing behavior needs more research and attention beyond the scope of the current paper. This motivates us to use $\langle H \rangle_{act} = 0.75$ for cases in Sections 4.2 and 4.4 as this has minimum estimation error over all *R*, as seen in Fig. 5.

In the following section, we intend to answer an interesting question—How robust is the *DFA* with respect to the presence of noise in linear $H(t)$?

4.4. Dependence on noise in $H(t)$

The robustness of *DFA* in the presence of noise is analyzed using a linear $H(t)$. We simulate *mBm* data using $H(t) = at + b + \epsilon_t$, where ϵ_t is drawn from Normal distribution ($\mathcal{N}(0, \sigma^2)$), and, *a* and *b* are the same as before. We control the strength of additive noise using parameter κ such that the standard deviation, $\sigma = \langle H \rangle_{act} \times \kappa = 0.75 \times \kappa$ for $\langle H \rangle_{act} = 0.75$ and $R = 0.06$. Other parameters, $p = 2$ and $T = 8192$ are the same as before and we average over 100 realizations of the data for each case.

From the results in Fig. 5, we see that $\langle H \rangle_{est}$ is very sensitive to κ, particularly to those values greater than 10^{-3} beyond which the relative accuracy falls far below the 5% limit of *EE*. We can see the threshold with respective to the reference green line which represents 95% of $\langle H \rangle_{act}$. It is interesting to note that while it is expected to have worsening performance with increasing κ, the rate of loss of accuracy for $\kappa \geq 10^{-3}$ is very high and goes to show how sensitive $\langle H \rangle_{est}$ is to noise in $H(t)$.

5. Conclusion

The characteristics of *DFA* in computing Hurst exponents from a non-stationary data with varying degrees of self-similarity (or *LRD*) are analyzed using *mBm* data. This is motivated mainly by increased use of *DFA* for real-life data, which more often than not is multifractional or with varying *H* [39–42]. We set out with a basic and intuitively meaningful assumption that the estimated exponent within reasonably slowly varying $H(t)$ is an average over time. This was shown to be true through numerical experiments on synthetic *mBm* data.

Furthermore, analysis of the effects of data and technique related parameters on the estimated exponent yielded some interesting insights and benchmarks for application of *DFA* on *mBm*. The following are the main conclusions on the usage of *DFA* technique for computing $H(t)$ using sliding window estimation or just estimate a time averaged Hurst exponent:

1. The order of polynomial, p used for detrending in *DFAp* has a limited and expected effect on our estimation as we see that even though *mBm* data is non-stationary, the non-stationarity is of a relatively simple kind and can be conveniently addressed by a lower order polynomial such as quadratic ($p = 2$). Application of *DFA* with $p > 2$ on *mBm* (and in general any data) should be done with caution due to poor conditioning of the higher order polynomial—more so in the lower time windows of estimation.
2. Data size (particularly greater than 2^{11}) does not predominantly affect the estimated exponent, although it would in general effect the precision (or standard error of least square fitting), more so due to limited number of averages performed in estimating the variance for fluctuation functions.
3. The range of the data, R which for a fixed data size controls the slope of $H(t)$ has a major effect on the accuracy of estimation. We find that $R = 0.06$ i.e., $H(t) = \langle H\rangle_{\text{act}} - \frac{R}{2} \rightarrow \langle H\rangle_{\text{act}} + \frac{R}{2}$ is a limiting condition for various data irrespective of $\langle H\rangle_{\text{act}}$. This conclusion is drawn on a 5% tolerance in *EE* as the limiting condition.
4. Increasing strength of additive noise diminishes the accuracy of estimation for obvious reasons. However, it is interesting to note how sensitive estimated exponents are with respect to the strength of noise. For a 5% tolerance in accuracy, we would desire that $H(t)$ have no more than $\langle H(t)\rangle \times 10^{-3}$ as standard deviation in noise. A noise of greater strength would quickly degrade the accuracy of the estimated exponents.

Beyond our observations on the nature of estimated exponents, we could also see a peculiar behavior of how *DFA* does a better job of estimating the time average of exponents when the data is predominantly self-similar ($H(t) \geq 0.7$). This phenomenon although interesting would require further study.

This work was supported by grants from NASA and National Science Foundation (NSF).

References

[1] B.B. Mandelbrot, Gaussian Self-Affinity and Fractals, Springer, New York, 2001.
[2] E. Koscielny-Bunde, A. Bunde, S. Havlin, H.E. Roman, Y. Goldreich, H. Schellnhuber, Indication of a universal persistence law governing atmospheric variability, Phys. Rev. Lett. 81 (1998) 729–732.
[3] E. Koscielny-Bunde, A. Bunde, S. Havlin, Y. Goldreich, Analysis of daily temperature fluctuations, Physica A 231 (1996) 393–396.
[4] J.D. Pelletier, D.L. Turcotte, Self-affine time series: 11. Applications and models, Adv. Geophys. 40 (1999) 91–166.
[5] R.O. Weber, P. Talkner, Spectra and correlations of climate data from days to decades, J. Geophys. Res. 106 (2001) 20131–20144.
[6] B.B. Mandelbrot, J.R. Wallis, Some long-run properties of geophysical records, Water Resour. Res. 5 (1969) 321–340.
[7] D. Koutsoyiannis, Climate change, the Hurst phenomenon, and hydrological statistics, Hydrol. Sci. J. 48 (2003) 3–24.
[8] C.-K. Peng, J. Mietus, J.M. Hausdorff, S. Havlin, H.E. Stanley, A.L. Goldberger, Long-range anticorrelations and non-Gaussian behavior of the heartbeat, Phys. Rev. Lett. 70 (1993) 1343–1346.
[9] C. Schäfer, M.G. Rosenblum, J. Kurths, H.H. Abel, Heartbeat synchronized with ventilation Heartbeat synchronized with ventilation, Nature 392 (1998) 239–240.
[10] J.W. Kantelhardt, T. Penzel, S. Rostig, H.F. Becker, S. Havlin, A. Bunde, Breathing during REM and non-REM sleep: correlated versus uncorrelated behaviour, Physica A 319 (2003) 447–457.
[11] A.S. Sharma, T. Veeramani, Extreme events and long-range correlations in space weather, Nonlinear Processes Geophys. 18 (2011) 719–725.
[12] H.E. Hurst, Long term storage capacity of reservoirs, Trans. Am. Soc. Eng. 116 (1951) 770–799.
[13] S. Karnel, V. Brendel, Patchiness and correlations in DNA sequences, Science 259 (1993) 677–680.
[14] H.E. Hurst, R.P. Black, Y.M. Simaika, Long-Term Storage, An Experimental Study, Constable, London, 1965.
[15] J.V. Sutcliffe, Obituary: Harold Edwin Hurst, Hydrol. Sci. J. 24 (1979) 539–541.
[16] C.-K. Peng, S.V. Buldyrev, S. Havlin, M. Simons, H.E. Stanley, A.L. Goldberger, Mosaic organization of DNA nucleotides, Phys. Rev. E 49 (1994) 1685–1689.
[17] R.M. Bryce, K.B. Sprague, Revisiting detrended fluctuation analysis, Sci. Rep. 2 (2012) 1–6.
[18] D. Horvatic, H.E. Stanley, B. Podobnik, Detrended cross-correlation analysis for non-stationary time series with periodic trends, Europhys. Lett. 94 (2011) 18007–18012.
[19] B.B. Mandelbrot, J.W. Van Ness, Fractional Brownian motions, fractional noises and applications, SIAM Rev. 10 (1968) 422–437.
[20] R.F. Peltier, J. Lévy-Véhel, Multifractional Brownian motion: definition and preliminary results, Rapport de Recherche de L'INRIA, No. 2645, 1995.
[21] J.A. Wanliss, P. Dobias, Space storm as a phase transition, J. Atmos. Sol.-Terr. Phys. 69 (2007) 675–684.
[22] A. Echelard, O. Barriere, J. Lévy-Véhel, Terrain modelling with multifractional Brownian motion and self-regulating processes, in: Computer Vision and Graphics 2010, Vol. 6374, 2010, pp. 342–351.
[23] S. Gaci, N. Zaourar, Heterogeneities characterization from velocity logs using multifractional Brownian motion, Arab. J. Geosci. 4 (2011) 535–541.
[24] S. Lennartz, A. Bunde, Distribution of natural trends in long-term correlated records: A scaling approach, Phys. Rev. E 84 (2011) 021129.
[25] D. Rybski, A. Bunde, On the detection of trends in long-term correlated records, Physica A 388 (2009) 1687–1695.
[26] J.W. Kantelhardt, S.A. Zschiegner, E. Koscielny-Bunde, S. Havlin, A. Bunde, H.E. Stanley, Multifractal detrended fluctuation analysis of nonstationary time series, Physics A 316 (2002) 87–114.
[27] A. Carbone, G. Castelli, H.E. Stanley, Time-dependent Hurst exponent in financial time series, Physica A 344 (2004) 267–271.
[28] H. Sheng, Y. Chen, T. Qiu, Tracking performance of Hurst estimators for multifractional Gaussian processes, in: Proceedings of FDA'10, The 4th IFAC Workshop Fractional Differentiation and its Applications, 2010.
[29] A. Kamont, On the fractional anisotropic Wiener field, Probab. Math. Statist. 16 (1996) 85–98.
[30] A.T.A. Wood, G. Chan, Simulation of stationary Gaussian processes in $[0, 1]^d$, J. Comput. Graph. Statist. 3 (1994) 409–432.
[31] P.J. Davis, Circulant Matrices, Wiley, New York, 1970.
[32] G. Chan, A. Wood, Simulation of multifractional Brownian motion, in: Proceedings in Computational Statistics, 1998.
[33] J.-F. Coeurjolly, (Ph.D. thesis), University Joseph Fourier, Grenoble, France, 2000.
[34] MATLAB code by Coeurjolly, J.-F. to generate mBm: http://www-ljk.imag.fr/SMS/software.html (Last update: 22 June 2001).
[35] J.W. Kantelhardt, E. Koscielny-Bunde, H.H.A. Rego, S. Havlin, A. Bunde, Detecting long-range correlations with detrended fluctuation analysis, Physica A 295 (2001) 441–454.
[36] V.A. Setty, (Ph.D. thesis), University of Maryland, College Park, Maryland, USA, 2014.
[37] R.H. McCuen, Statistical Methods for Engineers, Prentice Hall, Englewood Cliffs, NJ, 1985.

[38] M. Li, W. Zhao, Quantitatively investigating the locally weak stationarity of modified multifractional Gaussian noise, Physica A 391 (2012) 6268–6278.
[39] L. Hongre, P. Sailhac, M. Alexandrescu, J. Dubois, Nonlinear and multifractal approaches of the geomagnetic field, Phys. Earth Planet. Inter. 110 (1999) 157–190.
[40] J.A. Wanliss, D.O. Cersosimo, Scaling properties of high latitude magnetic field data during different magnetospheric conditions, in: International Conference Substorms—Vol. 8, 2006, pp. 325–329.
[41] H.L. Wei, S.A. Billings, M. Balikhin, Analysis of the geomagnetic activity of the D_{st} index and self-affine fractals using wavelet transforms, Nonlinear Processes Geophys. 11 (2004) 303–312.
[42] Rogério L. Costa, G.L. Vasconcelos, Long-range correlations and nonstationarity in the Brazilian stock market, Physica A 329 (2003) 231–248.